

4. Brittenham GM, Farrell DE, Harris JW, et al. Magnetic susceptibility of measurement of human iron stores. *N Engl J Med* 1982;307:1671.
5. Chapman RWG, Williams G, Bydder G, et al. Computed tomography for determining liver iron constant in primary haemochromatosis. *Br Med J* 1980;280:440.
6. Runge VM, Clanton JA, Smith FW, et al. Nuclear magnetic resonance of iron and copper disease states. *AJR* 1983;141:943.
7. Gorodetsky R, Goldfarb A, Dagan I, Rachmilewitz E. Noninvasive analysis of skin iron and zinc levels in beta-thalassemia major and intermedia. *J Lab Clin Med* 1985;105:44-51.
8. Metzger FR. Resonance fluorescence in nuclei. *Prog Nucl Phys* 1959;7: 54-88.
9. Vartsky D, Wielopolski L, Ellis KJ, Cohn SH. The use of nuclear resonant scattering of gamma rays for in vivo measurement of iron. *Nucl Instr Methods* 1982;193:350-364.
10. Wielopolski L, Vartsky D, Cohn SH. Application of nuclear resonance scattering for in vivo measurements. *Trans Am Nucl Soc* 1983;44:31-33.
11. Wielopolski L, Ancona RC, Mossey RC, Vaswani AN, Cohn SH. Nuclear resonance scattering measurement of human iron stores. *Med Phys* 1985; 12:401-404.
12. Modell B. Advances in the use of iron-chelating agents for the treatment for iron overload. *Progr Hematol* 1979;11:267-312.
13. Ackrill P, Ralston AJ, Day JP, Hodge KC. Successful removal of aluminum from patients with dialysis encephalopathy. *Lancet* 1980;27:692.
14. Brown DJ, Ham KN, Dawborn JK, Xipell JM. Treatment of dialysis osteomalacia with desferrioxamine. *Lancet* 1972;19:343-345.

CORRECTION

In the April issue of the *Journal*, Figures 1 and 3 in the article, "Detection of Bilateral and Symmetrical Anomalies in Technetium-99m-HMPAO Brain SPECT Studies," by Denays et al. were printed incorrectly. The corrected figures are shown below.

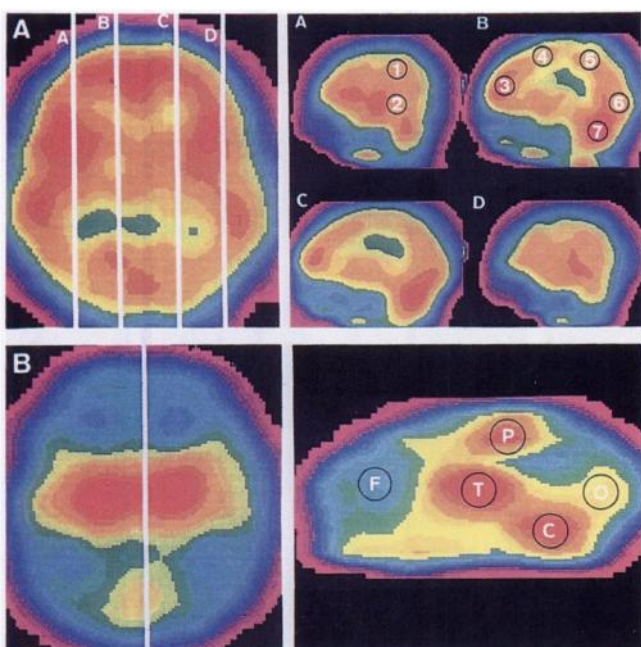


FIGURE 1. (A) In patients older than 1 mo, four sagittal slices, located at 25% (frame A), 40% (frame B), 60% (frame C) and 75% (frame D) of the width of the head, were used for the antero-posterior analysis of ^{99m}Tc-HMPAO SPECT studies. ROIs corresponded respectively to inferior motor (1), temporal (2), prefrontal (3), superior motor (4), parietal (5), occipital (6) and cerebellar (7) areas. (B) In neonates, for the antero-posterior analysis, tracer uptake was measured on the mediosagittal slice in frontal (F), parietal (P), occipital (O), thalamic (T) and cerebellar (C) areas.

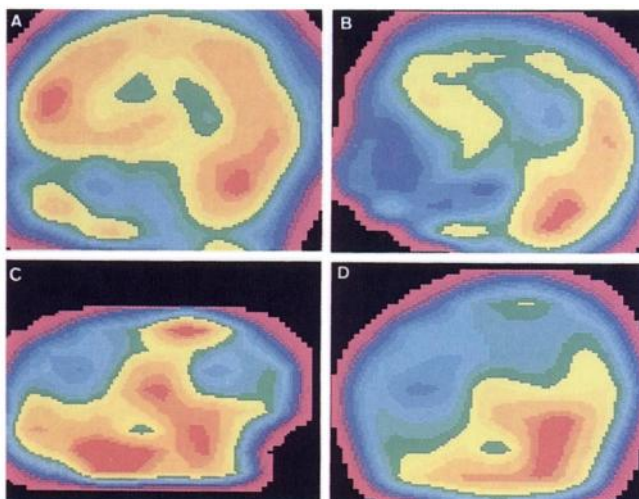


FIGURE 3. Sagittal ^{99m}Tc-HMPAO SPECT images obtained in two adults (A,B) and in two neonates (C,D). (A) A 25-yr-old "normal" adult with important tracer uptake in the cerebellum and in all cerebral cortical areas. (B) A 42-yr-old chronic alcoholic with decreased tracer uptake in the frontal and parietal cortices. (C) A "normal" neonate (gestational age of 40 wk) at the time of the SPECT study has prominent tracer uptake in the thalamic and cerebellar areas, while cerebral cortical regions, with the exception of primary sensorimotor cortex, are poorly visualized. (D) A neonate with diffuse hypotonia studied with SPECT at a gestational age of 42 wk has decreased tracer uptake in the thalamic area and sensorimotor cortex.